Proceedings of the ASME 2014 Dynamic Systems and Control Conference
DSCC2014
October 22-24, 2014, San Antonio, TX, USA

DSCC2014-6146

METHODOLOGY TO EVALUATE THE FUEL ECONOMY OF A MULTIMODE COMBUSTION ENGINE WITH THREE-WAY CATALYTIC CONVERTER

Sandro P. Nüesch*
Anna G. Stefanopoulou
University of Michigan
Ann Arbor, Michigan 48109
Email: snuesch@umich.edu

Li Jiang
Jeffrey Sterniak
Robert Bosch LLC
Farmington Hills, Michigan, 48331

ABSTRACT

Highly diluted, low temperature homogeneous charge compression ignition (HCCI) combustion leads to ultra-low levels of engine-out *NOx* emissions. A standard drive cycle, however, would require switches between HCCI and spark-ignited (SI) combustion modes. In this paper a methodology is introduced, investigating the fuel economy of such a multimode combustion concept in combination with a three-way catalytic converter (TWC). The TWC needs to exhibit unoccupied oxygen storage sites in order to show acceptable performance. But the lean exhaust gas during HCCI operation fills the oxygen storage and leads to a drop in *NOx* conversion efficiency. Eventually the levels of *NOx* become unacceptable and a mode switch to a fuel rich combustion mode is necessary in order to deplete the oxygen storage. The resulting lean-rich cycling leads to a penalty in fuel economy. In order to evaluate the impact of those penalties on fuel economy, a finite state model for combustion mode switches is combined with a longitudinal vehicle model and a phenomenological TWC model, focused on oxygen storage. The aftertreatment model is calibrated using combustion mode switch experiments from lean HCCI to rich spark-assisted HCCI and back. Fuel and emissions maps acquired in steady state experiments are used. Two depletion strategies are compared in terms of their influence on drive cycle fuel economy and *NOx* emissions.

1 INTRODUCTION

Two primary goals in current automotive industry and legislative focus are an increase in fuel economy and a reduction in emissions. One potential approach towards achieving both targets is advanced combustion technology. Homogeneous charge compression ignition (HCCI) has been an active topic in research for several years [1]. The compression ignition of gasoline leads to low temperature, flameless combustion and an increase in combustion efficiency due to reduced timing losses and improved mixture properties. In addition the chemical reactions producing *NOx* emissions are slowed down significantly. To avoid high pressure rise rates the charge requires strong dilution. Therefore the engine is run unthrottled, leading to an additional significant gain in fuel economy due to reduced pumping losses.

The operating regime of HCCI is limited to low and medium loads due to reduced combustion stability and increasing pressure rise rates, respectively. Even though during a standard drive cycle a substantial amount of time is spent within the HCCI operating regime [2] it is not possible to fulfill all the driver demands. A solution is the combination of HCCI with spark-ignited (SI) combustion in a multimode combustion approach [3]. However, as shown in [4, 5] this requires a large number of combustion mode switches. Due to the inherent differences between SI and

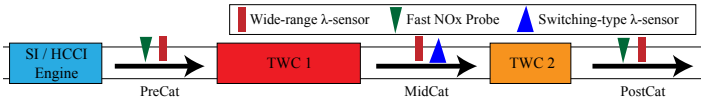

Figure 1: Setup for aftertreatment experiments and control.

*Address all correspondence to this author.

HCCI combustion, switches between those two modes are very difficult to control and exhibit a penalty in fuel consumption [6], depending on the applied hardware, actuator strategy, and operating condition. Combustion mode switches are discussed further in Section 5.

In order to fulfill the stringent emissions regulations an aftertreatment system is required. Three-way catalysts (TWC) are the main technology used to control emissions from gasoline engines. However, generally they are not suited for the application in lean-burn direct injection engine systems. TWCs require stoichiometric conditions in order to reduce NOx, HC, and CO simultaneously. In a lean environment selective catalyst reduction, lean de-NOx catalysts or NOx adsorbers can be used. Nevertheless, as mentioned above due to its low peak temperatures HCCI combustion leads to very low engine-out NOx emissions. Under lean HCCI conditions the TWC will still be able to convert CO and HC. In addition TWCs have the ability to store a limited amount of O_2 in order to compensate for variations in dilution. If the TWC's oxygen storage capacity (OSC) is sufficiently large, a high NOx conversion can be sustained for a certain amount of time while running lean HCCI. On the other hand if the OSC is filled the TWC needs to be depleted by running the engine rich which translates into a penalty in fuel economy.

Due to their wide distribution and relatively low cost the use of TWCs as aftertreatment system is desirable. Therefore this paper introduces a methodology to evaluate their impact on fuel economy within a SI-HCCI multimode concept; and to provide insight to the suitability of a TWC system as an afterteatment measure enabling high fuel economy and at the same time low emissions on a drive cycle.

An investigation of the trade-off between emissions and fuel economy in a SI-HCCI multimode engine is described in [7], based on experiments without drive cycle simulations. A different advanced combustion mode, reactivity controlled compression ignition (RCCI), is evaluated in terms of fuel economy and engine-out emissions by [8], using simulations and static maps. Similarly, this paper applies the longitudinal vehicle model explained and validated in [4] to show drive cycle fuel economy results. The methodology is extended by including steady-state emissions maps of the multimode engine, shown in Section 2. Mode switch experiments, explained in Section 3, are used to parameterize and validate a simple TWC and oxygen storage model in Section 4. The combustion mode switch model, shown in [2], is extended in Section 5 by accounting for rich SI combustion and emissions during the mode switches. In Section 6 two oxygen storage depletion strategies are introduced and their impact on drive cycle fuel economy and emissions is discussed in Section 7.

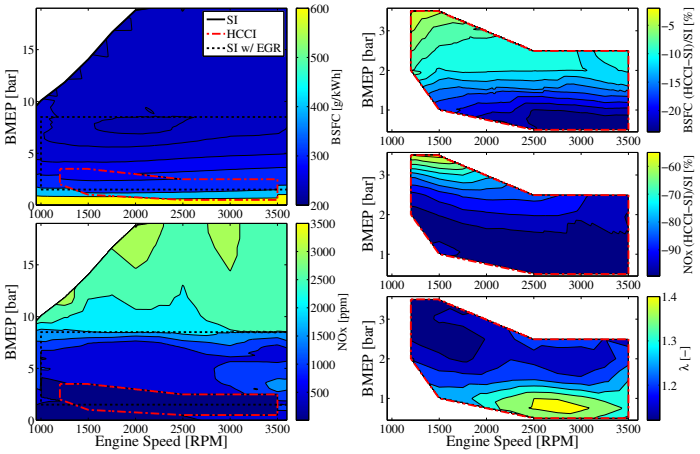

Figure 2: Maps of the multimode combustion engine based on experiments. Lean HCCI with low NOx (dash-dotted red), SI combined with eEGR (dotted black). Left: On top BSFC map and below engine-out NOx map. Right: Top and center show improvements in BSFC and NOx within the operating regime of HCCI compared to SI, respectively. Bottom: Map of rel. AFR λ.

2 HARDWARE & EXPERIMENTAL SETUP

2.1 Hardware

The engine used in this paper is a 2.0 L I4 multimode combustion engine with a compression ratio of 11.7:1. Engine bore and stroke are each 86 mm, the length of the connecting rod is 145.5 mm, and high and low cam lift are 10 and 4 mm, respectively. Due to increased compression ratio, 2-step cam profile switching, electric cam phasing for recompression, and stronger reciprocating components it is possible to run naturally aspirated (NA) HCCI besides the traditional SI mode. For control during nominal operation the aftertreatment system consists of three Emitec prototype TWC substrates with the first two substrates housed together in one can and the third packaged as an underfloor catalyst. The close coupled TWC substrates are based on Pd and $Pd+Rh$, and the underfloor TWC is based on $Pd+Rh$. The two catalysts each use a generous CeO_2-ZrO_2 oxygen storage. The hardware configuration is sketched in Fig. 1. The system is operated with two oxygen sensors (or λ-sensors). A wide-range sensor in front of the first catalyst and a switching-type sensor between the two catalysts. The hardware is discussed in more details in [7].

2.2 Experimental Setup

The sensors used for the experiments are also shown in Fig. 1. In addition to the wide-range λ-sensor in front of the first TWC two additional ones were placed between the two and after the second catalyst, respectively. Furthermore, the NOx emissions were measured using Cambustion CLD500 fast-NOx analyzers with a response time T_{10-90} of 10 ms. The space velocity was

approximately 13,000 l/hr.

SI-HCCI combustion mode switches require sophisticated control strategies. At the time of the experiments the 2-stage cam profile system and the control strategy were under development. Ideally a full switch would have been carried out during the experiments, including switches from low to high lift cams. Instead, using variable valve timing and a stoichiometric or rich air-fuel ratio (AFR), an extension strategy was tested with a switch to a mode described as spark-assisted HCCI (SA-HCCI) combustion. In this mode SI combustion conditions are approached but consisting of both flame propagation and some autoignition. Further information about spark-assisted compression ignition can be found in [9, 10]. More details about the experimental setup and results are described in [7].

3 EXPERIMENTS

3.1 Steady State

3.1.1 BSFC & Emission Maps In steady-state experiments maps of the multimode combustion engine were acquired, consisting of BSFC, relative AFR λ, and engine-out emissions over BMEP and engine speed ω_e, depicted in Fig. 2. In the following the maps are referred to as $NOx_{SI}(BMEP, \omega_e)$ and $NOx_{HCCI}(BMEP, \omega_e)$. As can be seen the use of HCCI leads to benefits in BSFC of more than 20% at low loads while it approaches SI values towards higher loads, where it operates much closer to stoichiometry. The very strong reduction in NOx emissions can be noticed as well, especially in the lower half of the operating regime. The HCCI regime overlaps with a region in which SI can be operated using external exhaust gas recirculation (eEGR). This strategy already results in a substantial decrease in NOx emissions. Nevertheless HCCI reduces those additionally by more than 95%.

The reader must note that in this paper only naturally aspirated (NA) HCCI is discussed. The advanced combustion regime can be extended by using multi-injection, multi-ignition (MIMI) strategies [11], SA-HCCI [12] or boosted HCCI [13].

3.1.2 Conversion Efficiency The conversion efficiency of the TWCs was measured at different dilutions and combustion modes, shown in Fig. 3. The engine was operated at 1800 RPM and between 1.6 bar and 3.1 bar BMEP. Under lean AFR conditions the TWC is ineffective in converting NOx, leading to equal pre- and post-cat NOx values. However, due to measurement errors the post-cat concentration may appear slightly larger than the pre-cat one, leading to negative conversion efficiencies. Therefore, for such cases zero conversion was assumed. As can be seen the static NOx conversion of the TWC is independent of the combustion modes. The fit is only a function of λ while other effects, such as temperature and chemical composition, were neglected.

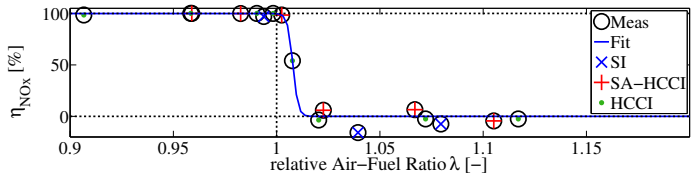

Figure 3: TWC NOx conversion efficiency measurements at 1800 RPM and fit (solid blue). SI (cross blue), SA-HCCI (plus red), HCCI (dot green).

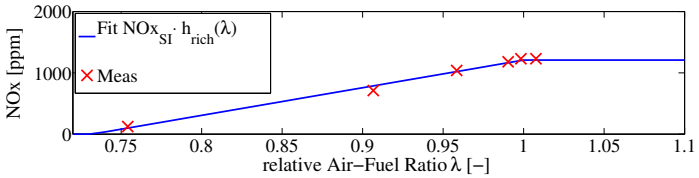

Figure 4: Steady-state NOx measurements at 1800 RPM (cross red) and linear fit (solid blue) over AFR.

Using the same experimental data a very basic approximation for the engine-out NOx emissions at rich conditions was found, shown in Fig. 4. In reality engine-out emissions during rich operation depend on many different factors. In strong simplification a function $h_{rich}(\lambda)$ is assumed to decrease the steady state NOx value proportionally to λ. Later on in the transient experiments and the simulations $\lambda = 0.9$ will be the most rich condition applied.

3.2 Transient Mode Switch

Combustion mode switches at different levels of dilution were investigated in order to characterize the two TWCs and their OSC. The combustion mode was switched between lean HCCI at $\lambda = \{1.06, 1.16, 1.34\}$ and rich SA-HCCI at $\lambda = \{0.9, 0.98\}$. The engine speed was kept constant at 1800 RPM and the load moved between 2 bar and 3 bar BMEP. During the combustion mode switches actuators settings such as intake and exhaust valve timing, injected fuel mass, and start of injection (SOI), were linearly moved between the steady-state settings during 1 s. It must be noted that this is not an optimized mode switch strategy and there might be potential to reduce the duration, efficiency and NOx emissions during the mode switch. In addition, as mentioned above, a complete mode switch to SI would involve switching the lift of the cams.

Experimental results of one particular run is shown in Fig. 5. As can be seen the oxygen storage delays the breakthrough of λ after the mode switches. As soon as the storage is full and λ_{post} switches to lean the conversion efficiency drops to zero and the NOx post-cat equals pre-cat. During the mode switches spikes in NOx occur before the values move to steady-state. Post-cat NOx continuously decreases to 0 ppm as the oxygen storage is being depleted and the TWC's conversion efficiency gradually increases.

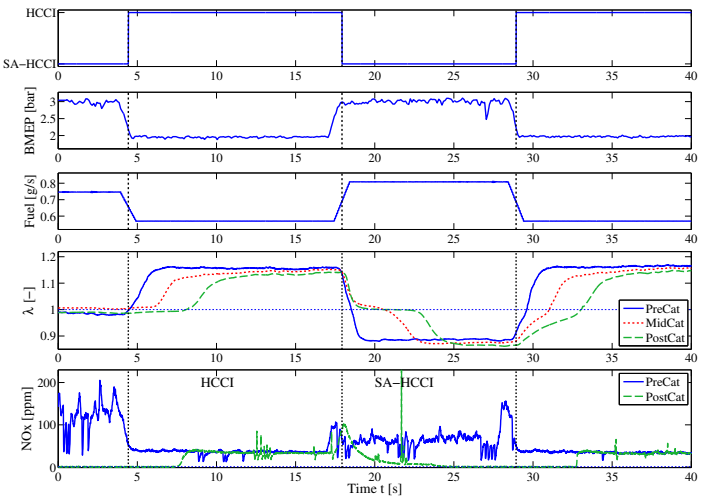

Figure 5: Combustion mode switch experiment between rich SA-HCCI ($\lambda = 0.9$) and lean HCCI ($\lambda = 1.16$). Top: Combustion mode based on EVC position. Second and third: BMEP and fuel mass flow command respectively. Fourth: Pre-cat AFR measurements (solid blue), mid-cat (dashed green) and post-cat (dotted red). Bottom: *NOx* measurements pre-cat (solid blue) and post-cat (dotted green).

Comparing these experimental results to examples published in literature (e.g. [14, 15]) a difference is apparent after the switch from SA-HCCI to HCCI. After the pre-cat AFR is changed from rich to lean, mid- and post-cat λ values are expected to show a fast response until they reach stoichiometry. Instead they exhibit a slow response. One possible explanation for this behavior might be the storage of hydrocarbons on the TWC during extensive rich operation. The hydrocarbons might get desorbed during the succeeding lean phase, leading to a rich post-cat λ.

4 OXYGEN STORAGE

4.1 Model

Modeling the chemical reactions occurring in a catalyst accurately requires detailed kinematic models [16, 17]. Nevertheless several approaches can be found in literature introducing simplifications to the system to make it more feasible for control-purposes. Those simplified models are either phenomenological and oxygen storage-dominated [18, 19] or based on reduced chemical relationships [14, 20]. They try to estimate the relative oxygen storage level, one of the most important states for aftertreatment control. In this paper the approach shown in [21, 22] is applied. In an effort to obtain an initial estimate of the fuel penalties due to emission constraints, the simple oxygen storage model was applied at all loads and speeds, extrapolating the behavior of the local conditions used for tuning the model.

The relative oxygen storage level Θ is the only state of the model, temperature dynamics are neglected. Inputs are air mass

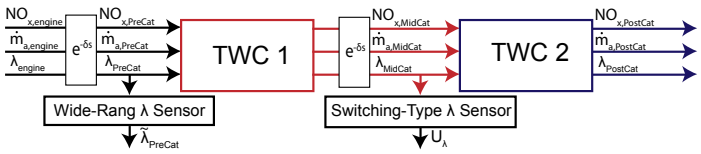

Figure 6: Block diagram of the system with the two TWCs and the two sensors.

flow $\dot{m}_a$, incoming *NOx* concentration and relative AFR λ_{in}. Outputs are outgoing *NOx* concentration and relative AFR λ_{out}. The reader is referred to [21, 22] for model equations and detailed explanations. Figure 6 shows the block diagram of the aftertreatment system with the two connected TWC blocks. The transport delays δ depend on ω_e. Also shown are the two sensors measuring λ_{PreCat} and λ_{MidCat}, resulting in $\tilde{\lambda}_{PreCat}$ and U_λ, respectively.

4.2 Validation

Six unknown parameters were found by matching the model to the transient mode switch experiments. Figure 7 shows the comparison of the model to the experiments. Steady-state map values at same speed / load conditions were used as inputs. Durations and behavior of λ during filling and depletion of the OSCs are very comparable. It can also be seen that both the steady-state *NOx* values match as well as the instant where the OSC is full and the conversion efficiency drops. Nevertheless this simplified model is not able to reproduce the two characteristics mentioned above, i.e. the immediate jump of $\lambda_{PostCat}$ to stoichiometry at $t = 30\,\mathrm{s}$ and the instantaneous drop of post-cat *NOx* to zero at $t = 18\,\mathrm{s}$. In addition since steady-state maps are used the *NOx* spikes are not recreated.

4.3 Estimation

It is not necessary to solely rely on the model in order to detect a deplete or full oxygen storage. The very accurate switching-type sensor, located between the two catalysts, provides feedback as soon as the AFR switches from lean to rich and vice versa. An approach shown by [23, 24] is adapted and integrated. The wide-range oxygen sensor in front of the first catalyst is modeled as a first order system with noise. In reality these sensors are also prone to biases which are neglected here.

An approximation, shown by [25], was used together with the λ-voltage characteristic of the implemented switching-type sensor. Voltage output U_λ is translated into an oxygen storage estimation $\hat{\Theta}_1$ by simply interpolating the signal in a narrow range around stoichiometry. A correctional input $\Delta\lambda$ is derived by comparing $\hat{\Theta}_1$ with the estimated $\tilde{\Theta}_1$ whenever λ_{MidCat} is close to stoichiometry. The integrator of the PI controller resets as soon as the gas composition deviates from stoichiometry. This model is almost equal to the one used as plant and shown in [21, 22]. Its parameters differ slightly from the ones of the model to include

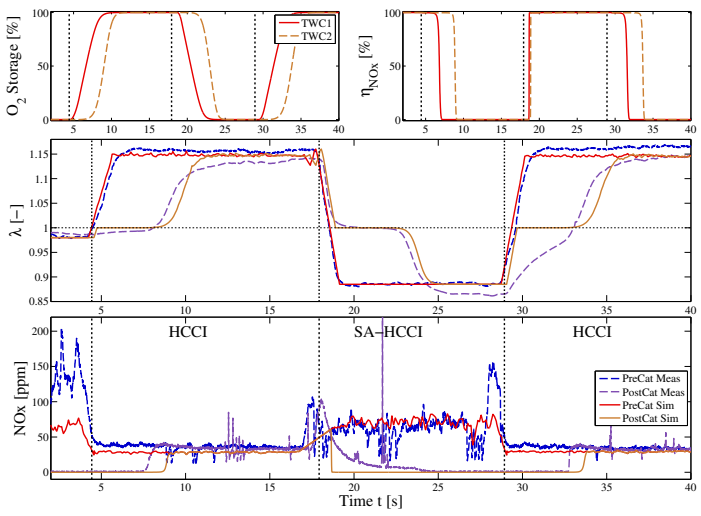

Figure 7: Validation of the aftertreatment model shown at same conditions as in Fig. 5. Top: Left and right plots of the OSC level and NOx conversion efficiency, respectively, for the two TWCs. Center and Bottom: Rel. AFR and NOx, respectively. Pre-cat and post-cat measurements (dashed dark and light blue, respectively). Pre-cat and post-cat simulation (solid red and orange, respectively).

some model uncertainty. Of course in combination with a more realistic plant, a parameter adaptation scheme as described by [24] is required to lead to good performance over the entire operating range.

5 COMBUSTION MODE SWITCH MODEL

5.1 Combustion Mode Switch

Above it was mentioned that controlling combustion mode switches between SI and HCCI is challenging. The reason being the large difference in their operating conditions. SI runs close to stoichiometry with positive valve overlap and a small amount of residual gas while HCCI runs lean with negative valve overlap and a significant amount of residuals. During a mode switch unstable regions need to be crossed leading to poor combustion work and a penalty in fuel economy [6], depending on operating conditions. Experimental studies are shown in [26, 27]; examples for control strategies can be found in [28, 29].

If instantaneous mode switches are assumed those effects are completely neglected and the BSFC map is simply changed accordingly. The penalization is implemented by using the finite state machine introduced in [2]. In this paper the model, depicted in Fig. 8, was extended to account for the influence of the aftertreatment system. Assumptions used for fuel penalties d_i during the mode switch are shown in Fig. 8. For more details it is referred to [2]. The model consists of 14 finite states at each time step k, represented by $M(k)$. The fuel beneficial combus-

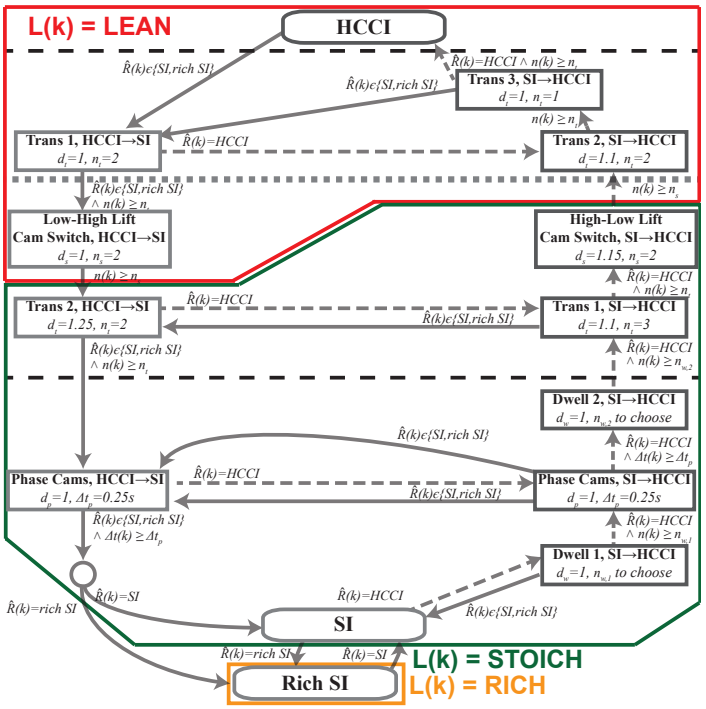

Figure 8: Finite state model of the combustion mode switch between SI and HCCI as shown in [2]. The *rich SI* combustion state was added. Depending on the control input r, $\hat{R}(k)$ denotes the currently BSFC-beneficial region or rich SI. The combustion modes were divided based on their dilution into $L(k) \in \{Stoich, Lean, Rich\}$. The number of cycles and the time since entering the current mode are denoted as states $n(k)$ and $\Delta t(k)$, respectively. The assumed parameters for fuel penalties d_i and durations n_i and Δt_i for each finite state i.

tion region is denoted $R(k) \in \{SI,\ HCCI\}$. This beneficial region can be understood as target of a mode switch. In addition to the previously published model, the binary control input r is used to command a switch to the rich SI mode. This leads to the modified region $\hat{R}(k) \in \{SI,\ HCCI,\ rich\ SI\}$, where rich SI is available as a target combustion region as well:

$$\hat{R}(k) = \begin{cases} rich\ SI & r(k-1) = true \\ R(k) & \text{else.} \end{cases} \quad (1)$$

5.2 Air-Fuel Ratio

Based on their dilution, all the finite states $M(k)$ are divided into subsets and labelled as $L(k) \in \{Stoich, Lean, Rich\}$, as can be seen in Fig. 8. For $L(k) = Stoich$ the engine-out AFR is assumed to be exactly stoichiometric without any deviations due to inaccuracies or AFR control. The value of λ, in case $L(k) = Rich$, is a control input. More fuel leads to a faster depletion of the

OSC but also higher fuel penalty. Here $\lambda = 0.9$ was chosen. For $L(k) = Lean$ the map output λ_{HCCI} from Fig. 2 is used. Therefore as long as $L(k)$ remains constant λ_{engine} is calculated as follows:

$$\lambda_{engine} = \begin{cases} 1 & L(k) = Stoich \\ 0.9 & L(k) = Rich \\ \lambda_{HCCI}(BMEP, \omega_e) & L(k) = Lean. \end{cases} \quad (2)$$

Changes from $L(k) = Stoich$ to $Rich$ or vice versa are assumed to be linear interpolations between the steady-state values during three engine cycles. Of course in reality the dilution during the combustion mode switches will strongly depend on the applied control strategy.

5.3 NOx

While $L(k) \in \{Stoich, Lean\}$ the engine-out NOx_{engine} is equal to the respective map values NOx_{SI} and NOx_{HCCI}. For $L(k) = Rich$ the SI map output is modified using the linear approximation function h_{rich},

$$NOx_{engine} = \begin{cases} NOx_{SI}(BMEP, \omega_e) & L(k) = Stoich \\ NOx_{SI}(BMEP, \omega_e) \cdot h_{rich}(\lambda_{engine}) & L(k) = Rich \\ NOx_{HCCI}(BMEP, \omega_e) & L(k) = Lean. \end{cases} \quad (3)$$

If $L(k)$ changes from Stoich to Rich or vice versa the NOx map is changed instantaneously. This is a strong assumption since depending on the control strategy and engine operating conditions spikes in NOx occur, as seen above.

6 DEPLETION STRATEGIES

In order to maximize fuel economy it is necessary to remain in the HCCI combustion mode for as long as possible while minimizing the total mode switch fuel penalty. On the other hand running lean HCCI eventually fills up the OSC and stops the conversion of NOx. Therefore the OSC must be depleted when returning to SI combustion by running the engine rich in order to avoid unacceptably high tailpipe NOx. Running rich SI obviously leads to an additional penalization of fuel economy.

In the following, two strategies are investigated in terms of fuel economy and NOx emissions. Figure 9 depicts a comparison of the strategies at an illustrative drive cycle situation.

6.1 Strategy: No Control of Oxygen Storage

In the first strategy the NOx emissions are completely neglected. There are no premature mode switches out of HCCI and also no oxygen storage depletions. Therefore the control value remains $r(k) = false$. This is an oversimplified strategy used

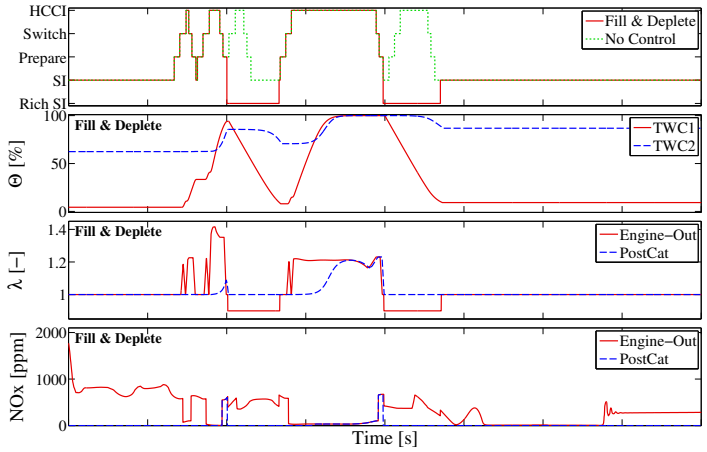

Figure 9: Depletion strategy *Fill & Deplete* at an example time interval during a drive cycle. Top: Currently active combustion mode. Intermediate modes from Fig. 8 summarized as Prepare and Switch. *No Control* strategy (dotted green) and *Fill & Deplete* strategy (solid red). Second: OSC trajectories for the *Fill & Deplete* strategy, TWC 1 (red) and TWC 2 (blue). Third: λ engine-out (red) and tailpipe (blue). Fourth: NOx engine-out (red) and tailpipe (blue).

in case if NOx levels during HCCI operation as well as mode switches are low enough to fulfill the emissions requirements. This will lead to the maximum drive cycle fuel economy. In reality, similar to a case after fuel cut-off events, some OSC depletion is always necessary to ensure high catalytic conversion, even in stoichiometric SI mode.

6.2 Strategy: Fill & Deplete after Mode Switch

The second strategy is a compromise between fuel economy and emissions. When the engine operates in HCCI mode $M(k) = HCCI$ the following conditions apply to the control value:

$$r(k) = \begin{cases} true & \tilde{\Theta}_1 > 0.9 \text{ AND } R(k) = SI \\ false & \text{else.} \end{cases} \quad (4)$$

Therefore a switch to rich SI is only demanded if OSC is estimated as full and the HCCI regime is left. The engine remains in depletion mode $M(k) = rich\ SI$ until the OSC is empty:

$$r(k) = \begin{cases} false & \tilde{\Theta}_1 = 0 \\ true & \text{else.} \end{cases} \quad (5)$$

As soon as this is the case a mode switch back to HCCI becomes possible again. In any other case $M(k) \notin \{rich\ SI, HCCI\}$ the control remains constant $r(k) = r(k-1)$.

This strategy leads to a fuel penalty due to the rich operation but should not substantially reduce the time spent in HCCI.

7 DRIVE CYCLE RESULTS

The strategies introduced above were applied in the federal test procedure (FTP-75) drive cycle simulation and compared to the SI-only case. Only the second and third phases of the FTP-75 were used since the temperature dynamics during cold start were neglected. The results are plotted in Fig. 10. They need to be treated with caution. As mentioned a large number of assumptions and simplifications were applied in the process.

Nevertheless it can be seen that the penalties due to the mode switches as well as the depletion have a very strong impact on fuel economy. Even if instantaneous mode switches are assumed it can be seen that the potential fuel economy benefits from using HCCI are negated entirely as soon as lean-rich cycling and succeeding OSC depletion phases are required.

As expected the SI-only case leads to the highest engine-out *NOx* but overall the difference between the strategies are relatively small. *NOx* spikes during mode switches might have a strong impact on the results. For tailpipe *NOx* the SI-only case leads to the lowest results by orders of magnitude due to the assumption of exact stoichiometry and perfect conversion. The first strategy without any oxygen storage control leads to the highest *NOx* emissions. Applying the mode switch fuel penalty leads to a reduction since time in HCCI is subtracted by the durations of the mode switches. Certainly this depends on the conditions during the mode switch. The use of the *Fill & Deplete* strategy leads to a strong reduction in tailpipe *NOx* emissions.

Shown is also the LEV II SULEV limit of 20 $^{mg}/_{mi}$ average tailpipe *NOx* emission during the FTP-75 drive cycle. As can be seen all the results, except for the SI-only case, are either very close to or over the limit. It has to be expected that in a more thorough analysis of the entire FTP-75 drive cycle the LEV II limits would be exceeded due to the following reasons: First, transient effects and possible *NOx* spikes have been neglected, leading to an increase in engine-out *NOx*. Second, the first phase of the FTP-75 drive cycle includes warm-up of the TWC. In general during this phase the largest portion of tailpipe *NOx* is produced. Third, exact stoichiometry and perfect *NOx* conversion are assumed in SI mode, which are simplifications as well. Together with the large penalty in fuel economy it can be concluded that a TWC aftertreatment system in a SI-HCCI multimode context is not suited for low emissions and requires an operation that reduces fuel efficiency.

8 CONCLUSION

A longitudinal vehicle model, a combustion mode switch state machine, and a phenomenological, oxygen storage dominated TWC model were combined in order to evaluate the fuel

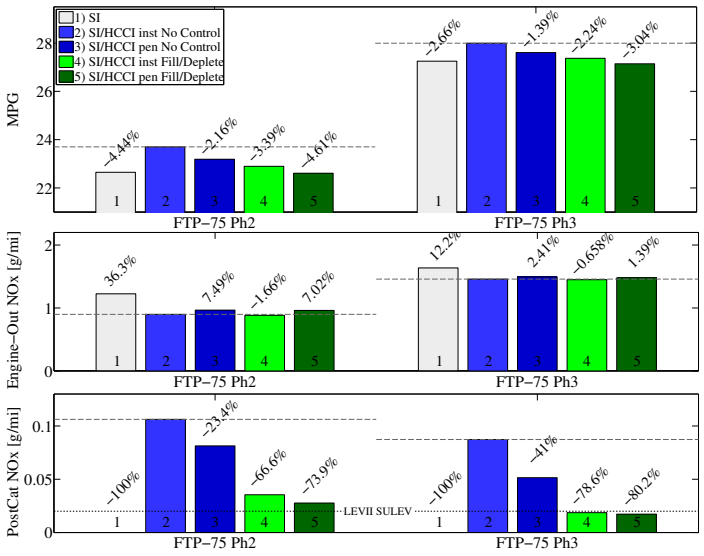

Figure 10: Drive cycle simulation results. Top: Fuel economy. Center: Average engine-out *NOx*. Bottom: Average tailpipe *NOx*. Two different oxygen storage depletion strategies were compared for instantaneous and penalized mode switches. For the penalties the assumptions shown in Fig. 8 were applied. Instantaneous case applying the strategy without control was used as baseline (dashed black). Results are compared to LEV II SULEV limit 20 $^{mg}/_{mi}$ (dotted black). Left and right for the second and third phases of the FTP-75, respectively.

economy and *NOx* emissions of a SI-HCCI multimode combustion engine on drive cycle level. The impact of two fuel penalties was investigated. The first one reflects directly the combustion conditions during the mode switches. The second one arises from the requirement of depleting the catalyst's oxygen storage by running the engine rich. Two illustrative aftertreatment strategies were compared, each targeting a different trade-off between fuel economy and emissions. It is shown that subsequent depletion of the TWC negates the fuel economy benefits gained during efficient HCCI operation. In addition low emissions standards for *NOx* were not robustly secured. SI-HCCI mode switch experiments at different operating conditions allow a more general characterization of fuel penalties, *NOx* spikes and AFR behavior. It is possible that the emissions problem can be circumvented if it is focused on stoichiometric combustion modes such as stoichiometric, spark-assisted HCCI. Moreover, SA-HCCI extends the operating regime of advanced combustion to higher loads compared to lean (NA) HCCI, hence its use will reduce the mode switches and thus the losses associated with the combustion mode switch. It is important to note, however, that the fuel efficiency of the SA-HCCI is not as high as the lean HCCI combustion, hence a thorough investigation is needed for the efficiency effectiveness of the stoichiometric version of HCCI.

ACKNOWLEDGMENT

This material is based upon work supported by the Department of Energy [National Energy Technology Laboratory] under Award Number(s) DE-EE0003533. This work is performed as a part of the ACCESS project consortium (Robert Bosch LLC, AVL Inc., Emitec Inc., Stanford University, University of Michigan) under the direction of PI Hakan Yilmaz and Co-PI Oliver Miersch-Wiemers, Robert Bosch LLC.

REFERENCES

[1] Thring, R., 1989. "Homogeneous charge compression ignition (HCCI) engines". In SAE Int. Fall Fuels and Lubricants Meeting and Exhibition.

[2] Nüesch, S., Hellström, E., Li, J., and Stefanopoulou, A., 2014. "Mode switches among SI, SACI, and HCCI combustion and their influence on drive cycle fuel economy". In ACC, pp. 849–854.

[3] Kulzer, A., Hathout, J.-P., Sauer, C., Karrelmeyer, R., Fischer, W., and Christ, A., 2007. "Multi-mode combustion strategies with CAI for a GDI engine". In SAE, no. 2007-01-0214.

[4] Nüesch, S., Hellström, E., Li, J., and Stefanopoulou, A., 2013. "Influence of transitions between SI and HCCI combustion on driving cycle fuel consumption". In ECC, pp. 1976–1981.

[5] Ortiz-Soto, E., Assanis, D., and Babajimopoulos, A., 2012. "A comprehensive engine to drive-cycle modelling framework for the fuel economy assessment of advanced engine and combustion technologies". *Int. J. Engine Res.,* **13**, pp. 287–304.

[6] Kakuya, H., Yamaoka, S., Kumano, K., and Sato, S., 2008. "Investigation of a SI-HCCI combustion switching control method in a multi-cylinder gasoline engine". In SAE, no. 2008-01-0792.

[7] Chen, Y., Sterniak, J., Sima, V., and Bohac, S., 2014. "Fuel efficiency and NOx reduction from multi-mode combustion with three-way catalysts". In ASME ICED Fall Technical Conference, submitted.

[8] Gao, Z., Curran, S., Daw, C., and Wagner, R., 2013. "Light-duty drive cycle simulations of diesel engine-out exhaust properties for an RCCI-enabled vehicle". In 8th U.S. National Combustion Meeting.

[9] Lavoie, G., Martz, J., Wooldridge, M., and Assanis, D., 2010. "A multi-mode combustion diagram for spark assisted compression ignition". *Combust. Flame,* **157**, pp. 1106–1110.

[10] Manofsky, D., Vavra, J., Assanis, D., and Babjimopoulou, A., 2011. "Bridging the gap between HCCI and SI: Spark-assisted compression ignition". In SAE, no. 2011-01-1179.

[11] Yun, H., Wermuth, N., and Najt, P., 2009. "Development of robust gasoline HCCI idle operation using multiple injection and multiple ignition (MIMI) strategy". In SAE, no. 2009-01-0499.

[12] Kalian, N., Zhao, H., and Yang, C., 2009. "Effects of spark-assistance on controlled auto-ignition combustion at different injection timings in a multicylinder direct-injection gasoline engine". *Int. J. Engine Res.,* **10**, pp. 133–148.

[13] Olsson, J.-O., Tunestal, P., and Johansson, B., 2004. "Boosting for high load HCCI". In SAE, no. 2004-01-0940, pp. 579–588.

[14] Tsinoglou, D., Koltsakis, G., and Peyton Jones, J., 2002. "Oxygen storage modeling in three-way catalytic converters". *Ind. Eng. Chem. Res.,* **41**, pp. 1152–1165.

[15] Peyton Jones, J. "Modeling combined catalyst oxygen storage and reversible deactivation dynamics for improved emissions prediction". In SAE, no. 2003-01-0999.

[16] Aimard, F., Li, S., and Sorine, M., 1996. "Mathematical modeling of automotive three-way catalytic converters with oxygen storage capacity". *Control Eng. Pract.,* **4**(8), pp. 1119–1124.

[17] Ohsawa, K., Baba, N., and Kojima, S. "Numerical prediction of transient conversion characteristics in a three-way catalytic converter". In SAE, no. 982556.

[18] Peyton Jones, J., Roberts, J., and Bernard, P. "A simplified model for the dynamics of a three-way catalytic converter". In SAE, no. 2000-01-0652.

[19] Muske, K., and Peyton Jones, J., 2004. "Estimating the oxygen storage level of a three-way automotive catalyst". In ACC.

[20] Kiwitz, P., Onder, C., and Guzzella, L., 2012. "Control-oriented modeling of a three-way catalytic converter with observation of the relative oxygen level profile". *J. Process Control*.

[21] Brandt, E., Wang, Y., and Grizzle, J., 2000. "Dynamic modeling of a three-way catalyst for SI engine exhaust emission control". *IEEE Trans. Contr. Syst. Technol.,* **8**(5).

[22] Fiengo, G., Grizzle, J., Cook, J., and Karnik, A., 2005. "Dual-UEGO active catalyst control for emissions reduction: Design and experimental validation". *IEEE Trans. Contr. Syst. Technol.,* **13**(5).

[23] Shafai, E., Roduner, C., and Geering, H. "Indirect adaptive control of a three-way catalyst". In SAE, no. 961038.

[24] Ammann, M., Geering, H., Onder, C., Roduner, C., and Shafai, E., 2000. "Adaptive control of a three-way catalytic converter". In ACC.

[25] Guzzella, L., and Onder, C., 2010. *Introduction to Modeling and Control of Internal Combustion Engine Systems*. Springer.

[26] Daw, S., Wagner, R., Edwards, D., and Green, J., 2007. "Understanding the transition between spark-ignited combustion and hcci in a gasoline engine". *Proc. Combust. Inst.,* **31**, pp. 2887–2894.

[27] Matsuda, T., Wada, H., Kono, T., Nakamura, T., and Urushihara, T., 2008. "A study of gasoline-fueled HCCI engine mode changes from SI combustion to HCCI combustion". In SAE, no. 2008-01-0050.

[28] Roelle, J., Shaver, M., and Gerdes, J., 2004. "Tackling the transition: A multi-mode combustion model of SI and HCCI for mode transition control". In Proc. of the ASME Dynamic Systems and Control Division.

[29] Yang, X., and Zhu, G., 2012. "SI and HCCI combustion mode transition control of an HCCI capable engine". *IEEE Trans. Contr. Syst. Technol.*

